ASIAN JOURNAL OF CIVIL ENGINEERING (BHRC) VOL. 17, NO. 6(2016)
PAGES 899-916

EXPERIMENTAL INVESTIGATION OF DAMAGED EXTERIOR RC BEAM–COLUMN JOINTS RETROFITTRD BY FRP JACKETING

E. Zamani Beydokhti and H. Shariatmadar*
Department of Civil Engineering, Faculty of Engineering, Ferdowsi University of Mashhad, Postal Code 9177948944, P.O. Box 1111, Mashhad, Iran

Received: 15 October 2015; **Accepted:** 25 January 2016

ABSTRACT

The efficiency of a seismic retrofit using externally bonded fiber-reinforced polymer composites on existing damaged reinforced concrete joints, designed prior to the introduction of modern standard seismic design code provisions in the mid-1970s, are herein presented, based on experimental investigations on beam-column joint subassemblies. The experimental program comprises 8 external beam–column joint connection subassemblages tested in 2 phases; the first phase was the damaging phase and the second was aimed to the repairing the damaged joints. The joints had no beam-column joint transverse reinforcement and special stirrups in beam and column critical lengths. These Non-Seismically designed (NS) joints were damaged with different levels at the first phase of the experiment. In the second phase, the damaged joints were strengthened with externally bonded carbon-fibre-reinforced plastics (C-FRP) sheets. From the observed responses the load carring capacity and stiffness of the pre-damaged strengthened joints were improved in moderate initial damages (less than 1.5% drift ratio). Also, the use of CFRP sheets increased the capacity of energy dissipation of the rehabilitated beam–column specimens in comparison to as-built specimen. It can be deduced that the technique of externally bonded retrofitting (EBR) using C-FRP sheets is efficient in moderately pre-damaged joints, i.e. the damage levels less than 1.5% drift ratio. This level is named as the repaire-ability level by using EBR strengthening method.

Keywords: Damaged RC beam-column joints; CFRP laminates; rehabilitation; performance level; ductility.

* E-mail address of the corresponding author: shariatmadar@um.ac.ir (Hashem Shariatmadar)

1. INTRODUCTION

Recent strong earthquakes in developing countries (Kashmir, 2005; China, 2008; Indonesia, 2009; and Haiti, 2010) caused extensive economic and human losses due to the poor behavior of many old reinforced concrete (RC) buildings The repair and rehabilitation of reinforced concrete structures damaged by severe earthquakes are challenging fields of study in earthquake engineering, which have been developed during the last two decades. lateral load carrying capacity of multi-storey reinforced concrete frames that were built prior to the 1970's are often insufficient due to non-ductile reinforcement detailing. Many failures in these structures can be attributed to the lack of internal steel stirrups in beam-column joints. Local strengthening of these deficient elements is a feasible option for reducing the vulnerability of such substandard buildings. On the other hand, the failure of these non-seismically designed joints may lead to general failure of the entire structure [1].

In the last two decades, externally bonded fiber-reinforced polymers (FRP) have been used extensively to strengthen seismically deficient elements. In comparison to other strengthening materials, FRP possess advantages such as high resistance to corrosion, excellent durability, high strength to weight ratio, adaptability to different shapes, and ease and speed of in situ application [2].

In the recent years, a lot of researches have been done on how using FRP laminates affect the behavior of the concrete joints [3-5]. There are also considerable experimental studies on the seismic parameters of the upgraded or repaired connections. Hadi and Tran [6] tested the exterior RC joint with joint shear (JS) failure, flexural beam hinge (BH) failure, and a combination of JS and BH failure mode. Lee et al. [7] investigated the effect of the simultaneously using of carbon and glass composites. Antonopoulos and Triantafillou [8] and Bing Li et al. [9] investigated the rehabilitation of the concrete connections with carbon and glass composites and compared the cyclic behaviors. Research of Balsamo et al. [10] about the effect of the CFRP laminates on the behavior of a full scale structure with dual system of moment frame and shear wall under cyclic and seismic loading have shown the improvement of the structural behavior. Garcia et al. [11] improved the strength of damaged joints by use of high strength concrete and CFRP laminates. Also, The tests carried out by Realfonzo et al. [12] on repaired joints have confirmed the efficiency of the strengthening solutions by use of CFRP sheets.

In this research, an effort to use carbon-fiber-reinforced plastic (CFRP) sheets in the improvement of the seismic parameters of reinforced concrete exterior beam–column joints is presented. Tested specimens were comprised of 8 external beam–column joint sub-assemblages having non-seismic reinforcement detailing with 2/3 scale tested in 2 phases; the first phase was the damaging phase and the second was aimed to the repairing the damaged joints. The joints had no beam-column joint transverse reinforcement and special stirrups in beam and column critical zones. These Non-Seismically designed (NS) joints were damaged up to the different levels at the first phase of the experiment. In the second phase, the damaged joints were strengthened with externally bonded carbon-fibre-reinforced polymers (CFRP) sheets. Therefore, the current tests aimed at (1) assessing behavior of substandard joints under different (moderate to severe) demands and (2) investigating effective rehabilitation and strengthening solutions for damaged joints with FRP sheets.

2. EXPERIMENTAL PROGRAM

2.1 Test specimen details

The beam of the joint subassemblage is taken to the mid-span of the bay, while the column is taken from the mid-height of one storey to the mid-height of the next storey. The sub-standard beam-column joint (NS5) was designed as per the current CSA A23.3-04 [13]. Beam and column cross sections with the 2/3 scale had the 30x40 cm and 30x30 cm dimensions, respectively. The length of the beam from mid span to the side of column was 1400 mm and the length of the column from the mid height of the bottom floor to the mid height of the higher floor was 2300 mm. The maximum-size coarse aggregate used in the concrete was 25 mm. The average compressive strength of concrete at the time of the test for all the specimens was 38.5 MPa. Also, The detailing of reinforcing in beam-column joint presented in Figure 1 is the same for all the specimens. Ø10 and Ø18 rebars, were used as stirrups and longitudinal reinforcement in the specimens. The material properties of used materials is presented in Table 1.

The longitudinal rebars for the columns were 8Ø18 bars corresponding to a 1.7% reinforcement ratio. The Ø10 stirrups were spaced at 200 mm over the entire height of the column. No transverse reinforcement was used in the joint area.

The top and bottom longitudinal reinforcements of the beam were 4Ø18 bars each corresponding to a 2.26% reinforcement ratio. The transverse reinforcement of the beam was Ø10 rectangular ties starting at 50 mm from the face of the column. The ties were spaced at 150 mm along the beam.

Table 1: Mechanical properties of materials

Tensile properties of reinforcement bars				
Rebar Diameter (mm)		F_y (MPa)		F_u (MPa)
Ø10		509.9		651.7
Ø18		533.3		696.0
Concrete Strength f'_c (MPa)				
NS5	NS1R	NS2R	NS3R	NS5R
38.5	38.9	38.6	38.6	38.5
FRP Materials				
	Thickness (mm)	Elongation %	Tensile Strength (MPa)	Tensile E-Modulus (GPa)	Areal Weight (gr/m^2)
CFRP: QUANTOM® Wrap 300C	0.167	1.5	4950	240	300
Epoxy resin	QUANTOM® EPR3301 epoxy laminating resin				

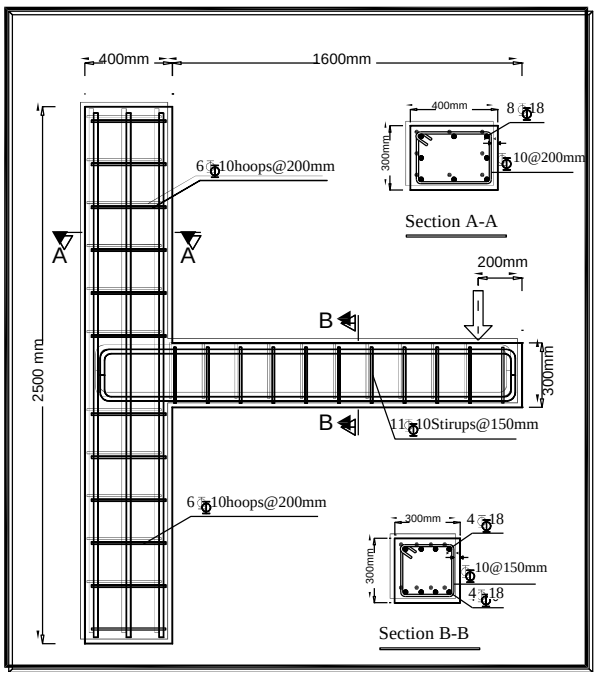

Figure 1. Reinforcing Detail of beam-column joint

2.2 Repaired specimens

Carbon fiber-reinforced polymer (CFRP) composite material was used to strengthen the joints after they had sustained extensive damage during Phase I testing. According to manufacturer data sheet, the tensile strength, elastic modulus, and ultimate strain of the CFRP sheets were presented in Table 1.

Based on the test results of specimen NS5 at the begining of the phase 1, the storey drifts corresponded to structural performance levels [Immediate Occupancy (IO), Life safety (LS) and Collapse Prevention (CP)] were obtained. The net beam rotation within 600 mm adjacent to column face was measured during the test according to FEMA 356 [14]. Thus, the tested NS-Grade specimens up to 1% (NS1), 1.5% (NS2) and 3% (NS3) storey drifts were selected for IO, LS and CP structural performance levels, respectively.

Based on previous researches on rehabilitation of connections [15, 16] and damage mechanism of NS5 specimen, the detailing shown in the Figure 2 was used for the repair of connections. Flexural retrofitting of Beam and column of the specimens were designed according to ACI440.2R-08 [17] presented in Table 2. Besides, the NS specimens was shear retrofitted using one layer sheet with the length of 500 mm on the two parallel sides of the column with the 90°angle relative to beam axis. Also, a 500 mm one layer U-shaped of the CFRP laminate on the three free faces of the joint with the 0°angle perpendicular to previous layer was attached to improve the confinement, strength and deformability of the joint.

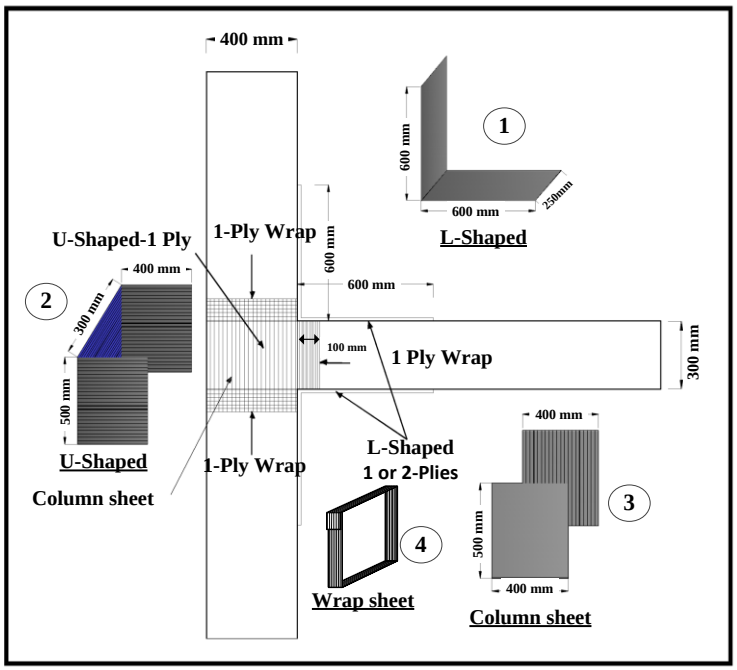

Figure 2. Application sequence and detailing of CFRP laminates

Table 2: Characteristics of retrofitted specimens

Joint ID	Pre-Loading (mm)	Ply Number of FRP Sheets		
		L-Shaped	U-Shaped	column Sheets
NS1R	(+14) , (-13)*	1	1	1
NS2R	(+20.8),(-20.2)	1	1	1
NS3R	(+44),(-42)	2	1	1
NS5R	(+71.2),(-71.3)	2	1	1

* (+) Forward loading, (-) Backward loading

2.3 Test set-up and loading history

The experimental setup for specimens is shown in Figure 3. The specimens were rotated 90° vertically, so the column placed on the floor of the laboratory and the beam was projected from the floor. The Figure 3 shows the fastened specimen on the strong floor.

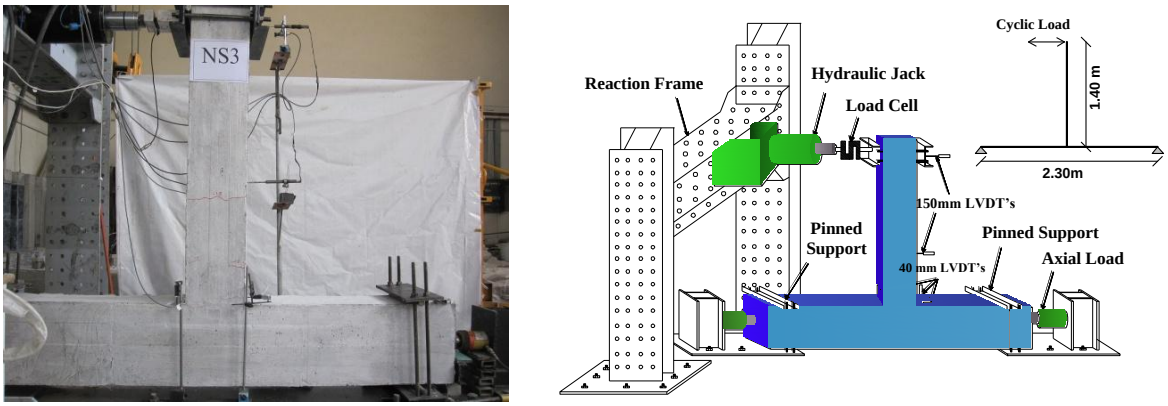

(a) (b)

Figure 3. Test set-up.

The end of beam and columns were points of contra flexure due to lateral loading of structure. The specimens were pin-supported at the mid height of the column connected to the reaction strong floor. A constant axial load about 70 kN was applied at the ends of column. Horizontal displacements were applied at beam mid span through a pin-ended double-acting 800 kN hydraulic actuator.

Five linear variable displacement transducers (LVDT) were used to measure the displacement at various locations on the specimen as shown in Figure 3-b. One 150-mm LVDT measured the beam tip displacement. Three 40 mm LVDTs were attached on the surface of beam and column at the vicinity of joint, and one 150 mm LVDT was mounted on the beam surface at a distance of 600 mm from column side for measuring the beam rotation and curvature.

Cyclic loading was applied to the tip of the beam according to the loading history displayed in Figure 4. Specimens were tested under a load-controlled cyclic in elastic range followed by displacement-controlled cyclic load history based on the inter-storey drift which represented a severe load condition for beam to column joint. The test loading pattern is based on drift rather than ductility increments because the ductility can be difficult to define for retrofitted systems other than conventionally reinforced concrete or steel structures.

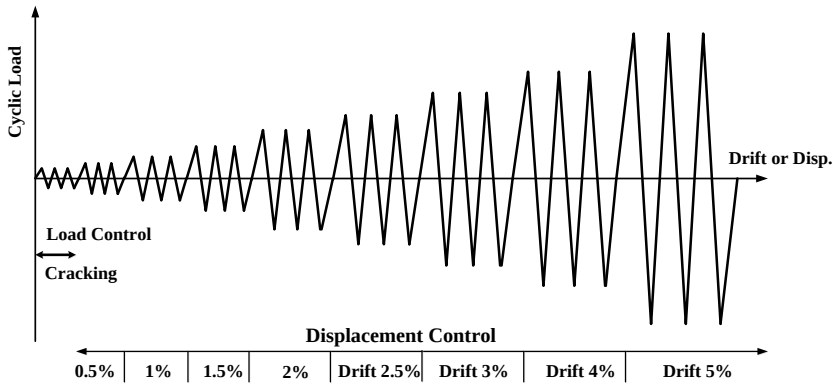

Figure 4. Load history for the reversed cyclic load test

3. TEST RESULTS

3.1 Phase I test results

NS5 specimen is the reference for specimens with non-seismic details. The test was started in elastic loading stage as load control. So, the loading was performed until the occurrence of the first bending crack on the beam in the vicinity of the column. The first bending crack appeared in the 15 kN load. After performing three repetitive cycles in this load, the load increased to 35 kN in the 0.5% drift. At this moment, the width of the bending crack was measured 0.7 mm. Increasing the load gradually, the structure entered the nonlinear behavior stage and loading was performed in the drifts 1%, 1.5%, 2%, 2.5% 3%, 4% and 5% respectively as shown in Fig. 5.

In the drift of 1.5%, bending cracks extended first in the 79 kN forward loading and then they extended in the backward loading along the longitudinal reinforcements. As approved after with the test results, the yielding of the beam's longitudinal reinforcement was occurred in 1.5% storey drift. At this moment, the crack's width increased to 1 mm. In the subsequent loading cycles in 90 kN load, diagonal cracks were created inside the joint and the width of the bending cracks increased to 2 mm. Finally, the width of these bending cracks was measured 6mm in the drift of 5%. At the end of the test in 86 kN load, the concrete in the compressive zone crushed on the beam and collapsed.

Due to the absence of transverse reinforcement confining the joint and also absence of special stirrup in the critical zones of the beam and column, diagonal cracks grew in the joint and concentrated in the beam's critical zone. The crack pattern in the last loading cycle and hysteresis curve of load-storey drift of NS5 specimen are displayed in Figure 5.

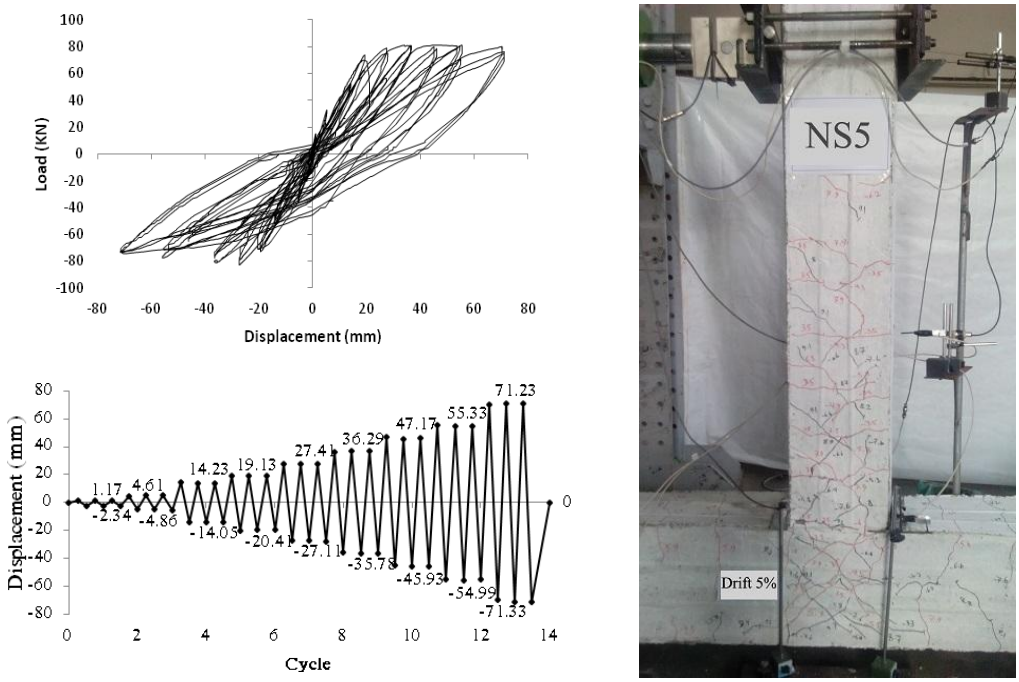

Figure 5. Hysteresis curve, loading history and crack pattern of specimen NS5

According to the NS5 specimen test results as will be presented in the next sections, the drifts 1%, 1.5% and 3% were obtained as the IO, LS and CP performance levels of the specimens based on FEMA 356 [14], respectively. Damage was applied on the specimens NS1, NS2 and NS3 so that the initial damages respectively equal to 1%, 1.5% and 3% be produced before strengthening. The geometrical characteristics and the materials used in the strengthened joints were exactly similar to NS5 specimen. The hysteresis curves of beam tip load-displacement for specimens NS1, NS2 and NS3 are plotted in Figure 6.

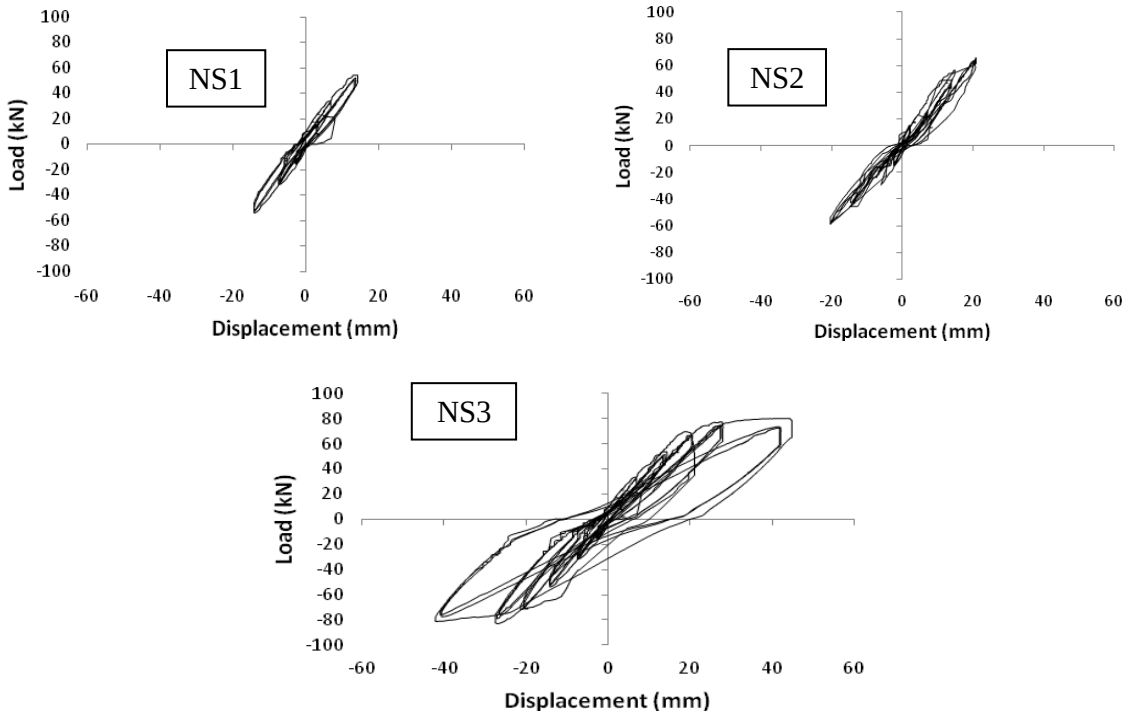

Figure 6. Hysteresis curves of specimens NS1, NS2 and NS3

3.2 Phase II test results

After finishing the first phase, the damaged specimens were strengthened and then were tested under reversed cyclic load, once more. The retrofitted specimens were named NS1R, NS2R, NS3R and NS5R. The NS1 specimen was experienced 1% storey drift in the first phase of experiment. The load was removed and then NS1 specimen was strengthened by one ply FRP sheet according to Figure 2 (specimen NS1R). Hysteresis curves for beam tip load-displacement of strengthened specimens are plotted in Figure 7. The load-carrying capacity of specimen NS1R increased up to an average 5% compared to the final capacity of NS5 specimen up to the drift 5% without any failure or separation of FRP layers.

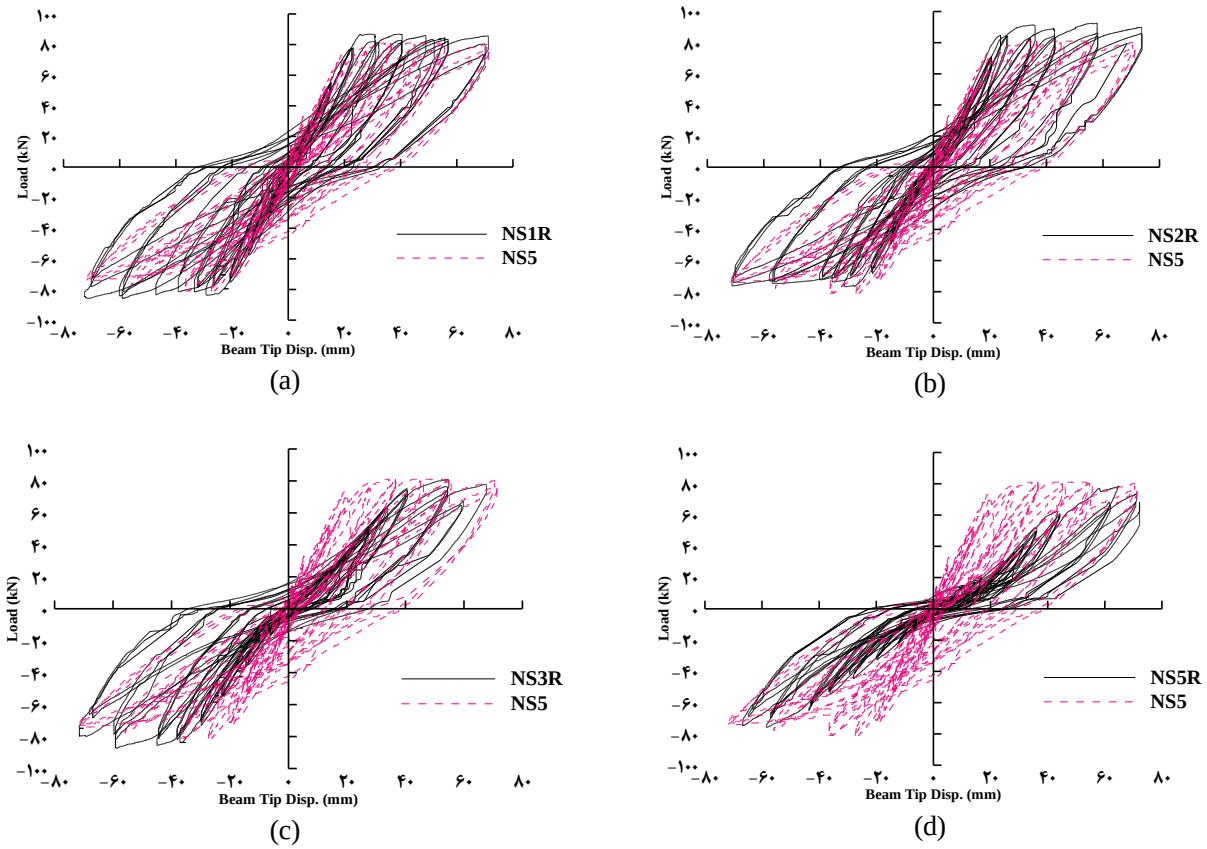

Figure 7. Load–displacement hysteresis curves of specimens

NS2 specimen was damaged to 1.5% storey drift in the first phase of experiment. The load was removed and NS2 specimen was strengthened by one ply FRP sheet under and above the beam and around the joint area according to Figure 2 (specimen NS2R). Similar to NS1R specimen according to Figure 7, NS2R specimen increased the load-carrying capacity on average to 3% compared to the ultimate capacity of NS5 specimen up to the drift 5% without any failure of FRP layers. In this specimen after the drift 2%, shear cracks extended from the end of the L-shaped FRP sheets top and bottom the beam. In the drift 3%, the L-shaped FRP layer buckled from the beam surfaces in several points. Finally, the L-shaped layer at the right hand side of the beam was then ruptured in the drift 4%. The crack pattern and FRP failure modes in tested specimens is presented in Figure 8.

Based on the test results of the NS5 specimen, it became clear that the drift 3% is equivalent to the last level of damage according to the Iranian seismic design provisions [18], at which the specimen can preserve its stability after a high damage . Hence, after the initial damage up to the 3% drift, NS3 specimen was unloaded and was then strengthened for bending by two FRP layers top and bottom of the beam and was shear strengthened by one layer around the joint (specimen NS3R).

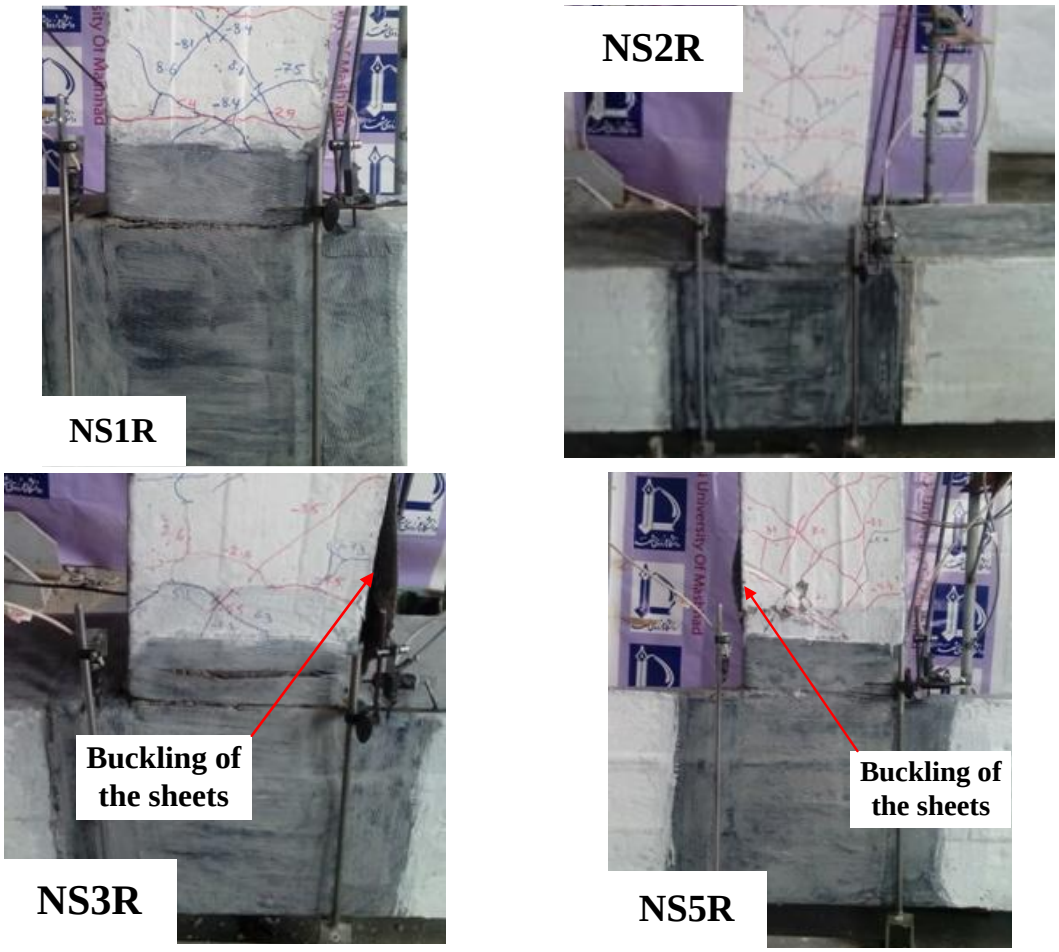

Figure 8. Crack pattern of strengthened specimens

Since the initial damage was high in specimen NS3R and despite the injection of epoxy mortar inside the opened cracks on the beam in the vicinity of the column, the cracks began to open very soon so that their width was measured 1.1 mm in the drift 2%. Increasing the load, the crack increased to 1.8 mm in the drift 2.5%, to 2mm in the drift 3% and to 5mm in the drift 4%. In addition in the drift 3%, L-shaped layers of the beam also buckled under compressive stresses and the wraps on the beam also tore at the corners. At the drift 4%, the L-shaped buckling increased and the wrap of the beam was completely cut. Although NS3R specimen recovered the joint's lost capacity and even tolerated 2% more than NS5 specimen, it must be mentioned that the NS3R specimen's behavior is smoother than the previous specimens that shows the reduction of stiffness and strength of the specimen compared to the previous reference and strengthened specimens (see Figure 7).

NS5R specimen had the highest level of damage up to 5% storey drift. After injecting wide cracks by epoxy mortar and strengthening by FRP layers, it was retested under reversed cyclic load.

The specimen's behavior was similar to NS3R specimen in terms of cracking but with a

higher intensity. At first in the drift 1%, bending cracks began to open in the vicinity of the column. In the drift 1.5%, L-shaped beams buckled from the surface in the vicinity of the wraps. The specimen's stiffness was significantly decreased by separation of the FRP L-shaped due to buckling. Then in the drift 2%, the compressive concrete crushed and the cracks above the L-shaped strength at the right hand side of the beam began to open. Finally in the drift 4%, L-shaped beams tore longitudinally. As it is displayed in Figure 7, the load-displacement curve of the specimen is more inclined than that of the previous specimens which caused the decrease of stiffness and strength of the NS5R specimen compared to the previous specimens. Also due to the slide of the beam's longitudinal reinforcements and separation of FRP from the concrete's surface, pinching was clearly observable.

The summary of load carrying capacity for specimens is presented in Table 3. According to the last column of Table 3, among the specimens that have achieved the capacity of the final drift 5%, only NS5R specimen has a lower load-carrying capacity than the basis NS5 specimen.

Table 3: Load carrying capacity of specimens in forward and backward loading

Joint ID	Maximum Storey Drift (%)	Forward Capacity (C+) (kN)	Backward Capacity (C-) (kN)	Ratio (+) (C/C_{NS5})	Ratio (-) (C/C_{NS5})	Mean Value
NS5 (base)	5	81.26	-82.98	1	1	1
NS1	1	53.95	-53.89	0.66	0.65	0.66
NS2	1.5	65.48	-58.4	0.81	0.7	0.75
NS3	3	80.5	-79.52	0.99	0.96	0.97
NS1R	5	86.75	-85.74	1.07	1.03	1.05
NS2R	5	92.41	-76.81	1.14	0.93	1.03
NS3R	5	80.87	-87.29	1	1.05	1.02
NS5R	5	78.3	-75.68	0.96	0.91	0.94

4. COMPARISON AND DISCUSSION OF TEST RESULTS

4.1 Capacity, secant stiffness and dissipated energy

To evaluate the effectiveness of the FRP sheets reinforcement, the strength, the stiffness, and the energy dissipation capacity for all cycles were recorded. The load carring capacity (maximum load) in both the push or the pull direction in the cycles regarded to 0.5%, 1.5%, 3% and 5% drift ratios were recorded as given in Table 4. The initial damage in different levels affected adversely the response of the strengthened joint. So, the repairing by the use of EBR method is less effective in pre-damaged joints. As seen in Table 4, the initial capacity was decreased in all strengthened joints compared with original joint (NS5). But when the FRP sheets activated in inelastic cycles (after 0.5% drift ratio), the capacity was exceeded in NS1R, NS2R and NS3R specimens respectively about 7%, 12% and 7% in compare with NS5 specimen. Only in NS5R (because of high per-damage level), the ultimate capacity decreased about 7%.

Secant stiffness can be introduced by the line between peak positive (or negative) direction and the origin of hysteresis loop in each loading cycle. Comparison of the repaired and original specimens showed an improvement in secant stiffness in the moderately damaged specimens. In the moderately damaged specimen, i.e. NS1R and NS2R, the secant stiffness of the repaired specimens were higher than the specimen NS5 about 25-50% after 0.5% drift ratio. The lower quality and compressive strength of damaged concrete in repaired specimens with higher pre-damage level than 1% can be the reason of decreasing in secant stiffness about 30-50%.

According the Table 4, the cumulative dissipated energy in repaired specimens was more than the original one at the end of the test; while the NS1R specimen showed more dissipated energy from the bigining due to less damage level. The results of this article are in line with those Panteladis et al. (2008). It was shown that the rehabilitation increased the dissipated energy of the beam–column specimens in comparison to as-built specimen from 20% in NS5R specimen to 235% in NS1R specimen.

Table 4: Comparison of seismic parameters of specimens

Seismic Parameter	Specimen ID	Drift Levels			
		0.50%	1.50%	3%	5%
Maximum Capacity (kN)	NS5	35.58	73.97	80.24	76.38
	NS1R	29.36	77.87	85.86	85.8
	NS2R	23.92	71.08	89.01	89.83
	NS3R	16.59	55.52	85.56	80.05
	NS5R	15.35	32.64	65.07	74.8
Secant Stiffness (kN/mm)	NS5	4.6	3.28	1.52	1.05
	NS1R	4	3.56	2.28	1.05
	NS2R	3.3	3.26	1.89	1.06
	NS3R	2.35	2.16	1.79	1.08
	NS5R	1.68	1.41	1.47	0.98
Dissipated energy (kJ)	NS5	0.21	2.15	6.91	14.18
	NS1R	0.33	2.86	20.86	48.02
	NS2R	0.14	1.52	14.42	43.56
	NS3R	0.15	1.53	9.66	28.52
	NS5R	0.2	0.95	5.48	16.92

4.2 Moment-curvature

Curvature and rotation at the joint and at the beam critical zone (distance of *2h* from the side of joint where *h* is the height of the beam cross section) were measured during the experiment. The beam section curvature was measured by the 150 mm LVDT installed at 600mm from the joint face in terms of the following formulation. Using curvature, the longitudinal strain can be obtained at the beam critical sections and the yield of reinforcements can be controlled.

If the displacement of the LVDT installed at *2h=600* mm from the joint face is denoted by Δ, it must be noted that the deformation resulted from the rotation of the joint must be subtracted from Δ value. This is done by reducing the rotation of the joint multiplied by *2h*. Assume that the rotation of the joint is θ_j, the beam's net displacement at 600 mm that is denoted by Δ_{net} is obtained from the Equation (1). If it can be assumed that the beam deforms as a circle in its critical zone, the circle radius (R) can be obtained from the circle Equation as Equation (2) and the curvature can be computed from 1/R (see Figure 9).

Using Equation (3), the circle radius can be determined and the beam curvature can be obtained by the Equation (4).

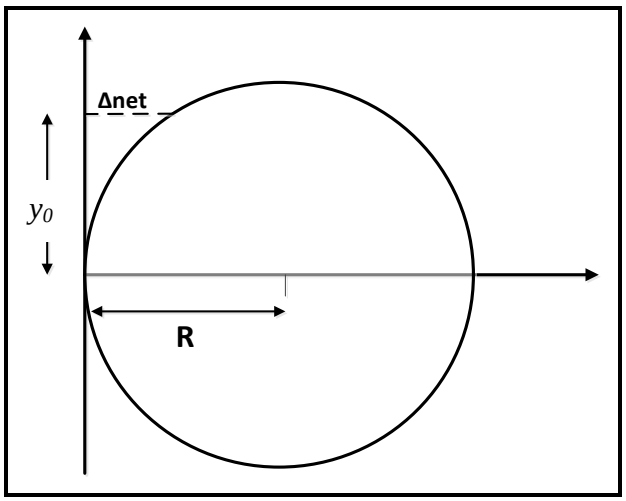

Figure 9. Circular deformation of beam and definition of R

$$\Delta_{net} = \Delta - 600\theta_j \tag{1}$$

$$(\Delta_{net} - R)^2 + y_0{}^2 = R^2 \tag{2}$$

$$R = \frac{\Delta_{net}{}^2 + y_0{}^2}{2\Delta_{net}} \tag{3}$$

$$\phi = \frac{1}{R} = \frac{2\Delta_{net}}{\Delta_{net}{}^2 + y_0{}^2} \tag{4}$$

where, R is the circle radius, y_0 is the critical length of the beam (2h) and ϕ is the curvature of beam section. Since the curvature is directly related to the strain, the beam strain at the vicinity of the joint can be obtained from the Equation (5).

$$\phi = \frac{\varepsilon}{c}$$
$$\varepsilon = \frac{2\Delta_{net}.C}{\Delta_{net}{}^2 + y_0{}^2} \tag{5}$$

where, ε is the section strain and C is the distance of any section string from the section neutral axis. Since the bending is symmetrically applied to the beam in two directions, it can be assumed that cracking is the same at both sides of the section and the neutral axis of the beam approximatelty remains in section middle axis.

According to the formulation that was mentioned above, moment-curvature curves are plotted in Figure 10. All strengthened specimens had a curvature more than reference specimen. As displayed in Figure 10, NS1R specimen has a higher load-carrying capacity and curvature than the NS5 specimen. In NS2R specimen, curvature is the same of specimen NS1R and its load-carrying capacity is higher than that of NS5 specimen. Higher strength in NS3R specimen did not reduce the curvature but increased the load-carrying capacity. Due to the higher damage of NS5R specimen, the curvature increased more than twice that of other strengthened specimens. Therefore, it is concluded that the retrofitting system increases the load-carrying and the curvature of the beam connected to the joint compared to the reference specimen.

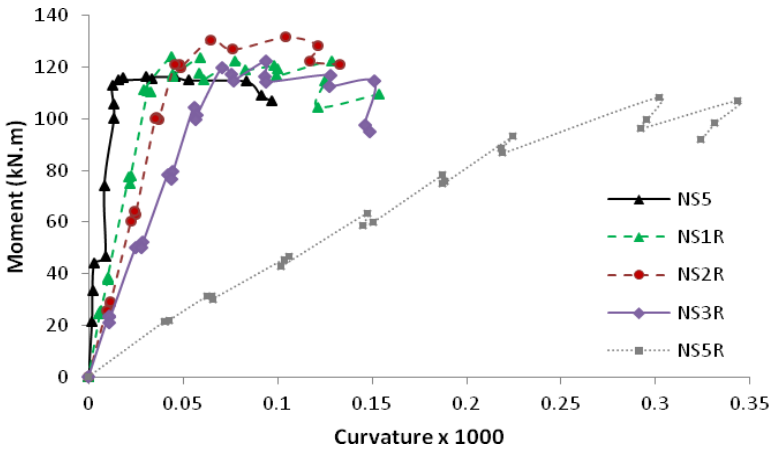

Figure 10. Moment – Curvature curve of beam's section.

4.3 Plastic rotation

The plastic rotation is plotted against moment and storey drift in separated curves of Figure 11. If the rotation in the elastic range is subtracted from the whole rotation, the plastic rotation will be obtained. This is performed in Excel spreadsheet program. Rotation is obtained at the core of the joint and in the beam critical zone by different LVDTs mounted in proper positions. Figure 11 shows that although all the tested joints had the same loading history, plastic rotation in the NS5 specimen beam was more than that of the strengthened specimens. In other words, strengthening the damaged joints by FRP layers, the plastic rotation of the joint and the damaged zones around it were decreased. This is due to the elastic nature of FRP materials. Also, Figure 11 shows that the plastic rotations of the beams in strengthened specimens were reduced in each storey drift in compared with reference specimen.

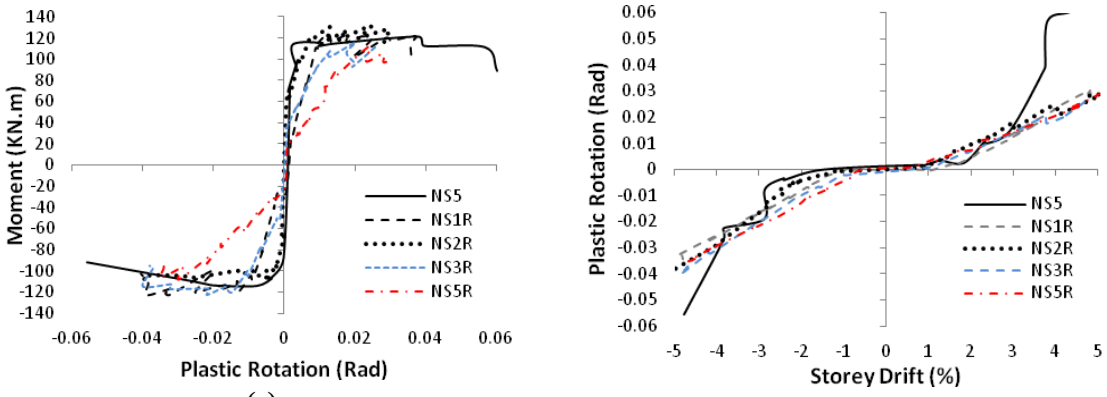

(a) (b)

Figure 11. Plastic rotation of the beam's plastic hinge

Since the structural performance levels are determined from the plastic rotation of beams and columns, beam and column plastic rotation-moment curves are used to evaluate of the joint performance levels in the following section.

4.4 Performance levels

Based on FEMA 356 [14] calculating the plastic rotation in the members, the damage levels can be computed. When the strengthening system can resist the plastic rotation up to the level of life safety without major decrease in the load-carrying capacity (less than 10%), the structure have acceptable performance. Analysis of the test results showed that the joint performance level is determined by the plastic hinge located in the end of the beam that is compatible with the weak beam-strong column theory.

The load capacity and storey drift related to each performance level of specimens is presented in Table 5. According to Table 5, the higher the specimen's capacity and drift are at any performance level, the more acceptable behavior is achieved. NS1R specimen retained the load-carrying capacity and the lateral displacement (drift) higher than those of the reference specimen at any level of performance. Also, NS2R specimen performed an acceptable behavior at any level of performance, especially in terms of the load-carrying capacity. NS3R had an acceptable behavior up to IO performance level. But since it had a higher initial damage than NS1R and NS2R specimens, it showed a lower load-carrying capacity after IO level. The performance levels of NS5R specimen occurred in lower capacity and drift compared with the reference specimen.

Table 5: Performance levels of tested B-C joints

Specimen ID	IO Level				LS Level				CP Level			
	Drift %	Capacity (kN.m)	Ratio to NS5		Drift %	Capacity (kN.m)	Ratio to NS5		Drift %	Capacity (kN.m)	Ratio to NS5	
			Drift	Capacity			Drift	Capacity			Drift	Capacity
NS5	0.44	43	1	1	1.82	107.35	1	1	3.07	115.15	1	1
NS1R	0.91	67	2.06	1.56	1.84	117	1.01	1.09	3.14	120	1.02	1.04
NS2R	0.65	46	0.72	1.07	1.43	101.47	0.78	0.95	2.75	120	0.81	1.04
NS3R	1.05	27	2.39	0.63	1.48	59	0.81	0.55	3.75	114	1.22	0.99
NS5R	0.63	19	1.43	0.44	1.36	35	0.75	0.33	3.1	86.95	1.01	0.76

Based on the results, it is proved that behavior of two strengthened specimens, i.e. NS1R and NS2R, improves the both performance level and load carrying capacity, simultaneously. Therefore, the damage level of beam-column connection up to 1.5% drift ratio is considered as the damage which can be repaired by strengthening using FRP laminates.

5. CONCLUSIONS

Eight 2/3-scale external RC beam-column joints were tested at the structural laboratory of the Ferdowsi University of Mashhad by simultaneously applying a constant axial load and lateral cyclic loading of increasing amplitudes. Tested specimens were comprised of five units tested in two phases. Testes joints had non-seismic reinforcement detailing, as is typical of pre-1970 Iranian construction practice before the introduction of seismic code provisions. C-FRP sheets were used to wrap the critical regions of the beam member and the joint panel zone of the examined sub-assemblages. Based on the experimental observations and data processing results, the following conclusions are drawn:

1- The results showed that the method is effective and capable of restoring or even upgrading load-carrying capacity and initial stiffness of damaged joints.
2- Comparison of the repaired and original specimens showed an improvement in secant stiffness in the moderately damaged specimens, i.e. NS1R and NS2R. Secant stiffness of these repaired specimens were higher than the specimen NS5 about 25-50% after 0.5% drift ratio.
3- It was shown that the rehabilitation increased the dissipated energy of the B-C joints in comparison to as-built specimen from 20% in NS5R specimen to 235% in NS1R specimen.
4- The performance level of damaged joints under cyclic tests was improved. it is deduced that behavior of two strengthened moderately damaged specimens, i.e. NS1R and NS2R, improves the both performance level and load carrying capacity, simultaneously.
5- The repair ability level of damage was also evaluated up to 1.5% drift ratio for tested B-C joints. Nevertheless, the plastic rotation of critical beam section and joint was decreased due to elastic nature of FRP materials.

NOTATIONS

h: Depth of section

Δ: The displacement at $2h=600$ mm from the joint face

θ_j: The rotation of the joint

Δ_{net}: The beam's net displacement at 600 mm

R: Circle radius if the beam's deformed shape could be assumed as a circle in its critical zone

y_0: The critical length of the beam ($2h$)

ϕ: The curvature of beam's section

ε : The section strain
C: The distance of any section fiber from the section neutral axis
Φ : Deformed bar
θ_y : Rotation at general yielding state of the joint
θ_u : Rotation at general ultimate state of the joint
δ_y : Displacement at general yielding state of the joint
δ_u : Displacement at general yielding state of the joint

REFERENCES

1. Park R, Paulay T. Reinforced Concrete Structures, Wiley, New York, 1975
2. Rizkalla S, Hassan T, Hassan N. Design recommendations for the use of FRP for reinforcement and strengthening of concrete structures, *Progress in Structural Engineering and Materials*, No. 1, **5**(2003) 16-28.
3. Vatani-Oskouei A. Repairing of seismically damaged RC exterior beam-column connection using CFRP, *Journal of Reinforced Plastics and Composites*, 2010.
4. Almusallam TH, Elsanadedy HM, Al-Salloum YA, Alsayed SH. Experimental and numerical investigation for the flexural strengthening of rc beams using near-surface mounted steel or GFRP bars, *Construction and Building Materials*, **40**(2013) 145-61.
5. Del Vecchio C, Di Ludovico M, Balsamo A, Prota A, Manfredi G, Dolce M. Experimental investigation of exterior RC beam-column joints retrofitted with FRP systems, *Journal of Composites for Construction*, No. 4, **18** (2014) 04014002.
6. Hadi MN, Tran TM. Seismic rehabilitation of reinforced concrete beam–column joints by bonding with concrete covers and wrapping with FRP composites, *Materials and Structures*, (2014) 1-19.
7. Li J, Samali B, Ye L, Bakoss S. Behaviour of concrete beam–column connections reinforced with hybrid FRP sheet, *Composite Structures*, No. 1, **57**(2002) 357-65.
8. Antonopoulos CP, Triantafillou TC. Analysis of FRP-strengthened RC beam-column joints, *Journal of Composites for Construction*, No. 1, **6**(2002) 41-51.
9. Li B, Kai Q. Seismic behavior of reinforced concrete interior beam-wide column joints repaired using FRP, *Journal of Composites for Construction*, No. 3, **15**(2010) 327-38.
10. Balsamo A, Colombo A, Manfredi G, Negro P, Prota A. Seismic behavior of a full-scale RC frame repaired using CFRP laminates, *Engineering Structures*, No. 5, **27**(2005) 769-80.
11. Garcia R, Jemaa Y, Helal Y, Guadagnini M, Pilakoutas K. Seismic strengthening of severely damaged beam-column RC joints using CFRP, *Journal of Composites for Construction*, No. 2, **18**(2013).
12. Realfonzo R, Napoli A, Pinilla JGR. Cyclic behavior of RC beam-column joints strengthened with FRP systems, *Construction and Building Materials*, **54**(2014) 282-97.
13. Association CS. Design of concrete structures, CSA A23. 3-04, CSA, Rexdale, Ontario, 2004.
14. FEMA356. Prestandard and Commentary for the Seismic Rehabilitation of Buildings: Rehabilitation Requirement s. American Society of Civil Engineers Washington, DC, 2000.
15. Ilki A, Bedirhanoglu I, Kumbasar N. Behavior of FRP-retrofitted joints built with plain bars

and low-strength concrete, *Journal of Composites for Construction*, No. 3, **15**(2010) 312-26.
16. Pantelides CP, Okahashi Y, Reaveley L. Seismic rehabilitation of reinforced concrete frame interior beam-column joints with FRP composites, *Journal of Composites for Construction*, No. 4, **12**(2008) 435-45.
17. ACI440.2R-08. Guide for the design and construction of externally bonded FRP system for strengthening concrete structures, in ACI 440.2R-08, Michigan (USA), 2008.
18. Iranian Code of Practice for Seismic Resistant Design of Buildings, Standard No.2800, Building and housing research center (BHRC), 2005.